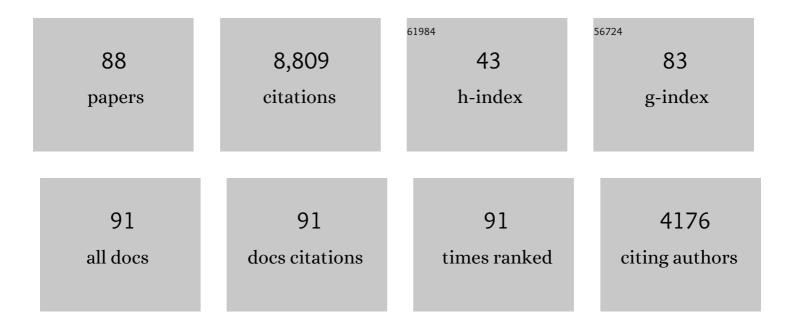
## Victoria E Hamilton

List of Publications by Year in descending order

Source: https://exaly.com/author-pdf/1760942/publications.pdf Version: 2024-02-01



#	Article	IF	CITATIONS
1	Mid-infrared emissivity of partially dehydrated asteroid (162173) Ryugu shows strong signs of aqueous alteration. Nature Communications, 2022, 13, 364.	12.8	10
2	Linear Modeling of Spectra of Fine Particulate Materials: Implications for Compositional Analyses of Primitive Asteroids. Earth and Space Science, 2022, 9, .	2.6	1
3	Olivine and carbonate-rich bedrock in Gusev crater and the Nili Fossae region of Mars may be altered ignimbrite deposits. Icarus, 2022, 380, 114974.	2.5	8
4	Nanoâ€FTIR Investigation of the CM Chondrite Allan Hills 83100. Journal of Geophysical Research E: Planets, 2022, 127, .	3.6	2
5	Assessing the Sampleability of Bennu's Surface for the OSIRIS-REx Asteroid Sample Return Mission. Space Science Reviews, 2022, 218, 20.	8.1	12
6	GRO 95577 (CR1) as a mineralogical analogue for asteroid (101955) Bennu. Icarus, 2022, 383, 115054.	2.5	6
7	Highâ€Resolution Thermophysical Analysis of the OSIRISâ€REx Sample Site and Three Other Regions of Interest on Bennu. Journal of Geophysical Research E: Planets, 2022, 127, .	3.6	5
8	Spacecraft sample collection and subsurface excavation of asteroid (101955) Bennu. Science, 2022, 377, 285-291.	12.6	39
9	Spectral analysis of craters on (101955) Bennu. Icarus, 2021, 357, 114252.	2.5	6
10	Meteoritic evidence for a Ceres-sized water-rich carbonaceous chondrite parent asteroid. Nature Astronomy, 2021, 5, 350-355.	10.1	10
11	Exogenic basalt on asteroid (101955) Bennu. Nature Astronomy, 2021, 5, 31-38.	10.1	57
12	Spectral Characterization of Bennu Analogs Using PASCALE: A New Experimental Setâ€Up for Simulating the Nearâ€Surface Conditions of Airless Bodies. Journal of Geophysical Research E: Planets, 2021, 126, e2020JE006624.	3.6	10
13	The Role of Hydrated Minerals and Space Weathering Products in the Bluing of Carbonaceous Asteroids. Planetary Science Journal, 2021, 2, 68.	3.6	14
14	In search of Bennu analogs: Hapke modeling of meteorite mixtures. Astronomy and Astrophysics, 2021, 648, A88.	5.1	9
15	Evidence for limited compositional and particle size variation on asteroid (101955) Bennu from thermal infrared spectroscopy. Astronomy and Astrophysics, 2021, 650, A120.	5.1	30
16	Spectrophotometric Modeling and Mapping of (101955) Bennu. Planetary Science Journal, 2021, 2, 117.	3.6	9
17	A Novel Atmospheric Removal Technique for TES Spectra Applied to Olivine and Carbonateâ€Rich Bedrock in the Nili Fossae Region, Mars. Journal of Geophysical Research E: Planets, 2021, 126, e2021JE006822.	3.6	5
18	Lucy Mission to the Trojan Asteroids: Science Goals. Planetary Science Journal, 2021, 2, 171.	3.6	54

#	Article	IF	CITATIONS
19	Lucy Mission to the Trojan Asteroids: Instrumentation and Encounter Concept of Operations. Planetary Science Journal, 2021, 2, 172.	3.6	21
20	Composition of organics on asteroid (101955) Bennu. Astronomy and Astrophysics, 2021, 653, L1.	5.1	10
21	Machine Learning Midâ€Infrared Spectral Models for Predicting Modal Mineralogy of CI/CM Chondritic Asteroids and Bennu. Journal of Geophysical Research E: Planets, 2021, 126, e2021JE007035.	3.6	11
22	Heterogeneous mass distribution of the rubble-pile asteroid (101955) Bennu. Science Advances, 2020, 6, .	10.3	50
23	Widespread carbon-bearing materials on near-Earth asteroid (101955) Bennu. Science, 2020, 370, .	12.6	56
24	Bright carbonate veins on asteroid (101955) Bennu: Implications for aqueous alteration history. Science, 2020, 370, .	12.6	71
25	Variations in color and reflectance on the surface of asteroid (101955) Bennu. Science, 2020, 370, .	12.6	84
26	Asteroid (101955) Bennu's weak boulders and thermally anomalous equator. Science Advances, 2020, 6,	10.3	83
27	Signatures of the post-hydration heating of highly aqueously altered CM carbonaceous chondrites and implications for interpreting asteroid sample returns. Geochimica Et Cosmochimica Acta, 2020, 289, 69-92.	3.9	15
28	Effects of small crystallite size on the thermal infrared (vibrational) spectra of minerals. American Mineralogist, 2020, 105, 1756-1760.	1.9	13
29	OSIRIS-REx spectral analysis of (101955) Bennu by multivariate statistics. Astronomy and Astrophysics, 2020, 637, L4.	5.1	23
30	Visible–near infrared spectral indices for mapping mineralogy and chemistry with <scp>OSIRIS</scp> â€ <scp>RE</scp> x. Meteoritics and Planetary Science, 2020, 55, 744-765.	1.6	7
31	Phase reddening on asteroid Bennu from visible and near-infrared spectroscopy. Astronomy and Astrophysics, 2020, 644, A142.	5.1	22
32	Weak spectral features on (101995) Bennu from the OSIRIS-REx Visible and InfraRed Spectrometer. Astronomy and Astrophysics, 2020, 644, A148.	5.1	22
33	The first samples from Almahata Sitta showing contacts between ureilitic and chondritic lithologies: Implications for the structure and composition of asteroid 2008 <scp>TC</scp> <sub>3</sub> . Meteoritics and Planetary Science, 2019, 54, 2769-2813.	1.6	32
34	Evidence for widespread hydrated minerals on asteroid (101955) Bennu. Nature Astronomy, 2019, 3, 332-340.	10.1	251
35	Properties of rubble-pile asteroid (101955) Bennu from OSIRIS-REx imaging and thermal analysis. Nature Astronomy, 2019, 3, 341-351.	10.1	188
36	The unexpected surface of asteroid (101955) Bennu. Nature, 2019, 568, 55-60.	27.8	364

#	Article	IF	CITATIONS
37	Thermal Infrared Spectral Analyses of Mars from Orbit Using the Thermal Emission Spectrometer and Thermal Emission Imaging System. , 2019, , 484-498.		1
38	Thermal Infrared Remote Sensing of Mars from Rovers Using the Miniature Thermal Emission Spectrometer. , 2019, , 499-512.		1
39	The Thermophysical Properties of the Bagnold Dunes, Mars: Groundâ€Truthing Orbital Data. Journal of Geophysical Research E: Planets, 2018, 123, 1307-1326.	3.6	34
40	The OSIRIS-REx Thermal Emission Spectrometer (OTES) Instrument. Space Science Reviews, 2018, 214, 1.	8.1	94
41	Shergottite Northwest Africa 6963: A Pyroxeneâ€Cumulate Martian Gabbro. Journal of Geophysical Research E: Planets, 2018, 123, 1823-1841.	3.6	20
42	Visible/nearâ€infrared spectral diversity from in situ observations of the Bagnold Dune Field sands in Gale Crater, Mars. Journal of Geophysical Research E: Planets, 2017, 122, 2655-2684.	3.6	40
43	Chemistry, mineralogy, and grain properties at Namib and High dunes, Bagnold dune field, Gale crater, Mars: A synthesis of Curiosity rover observations. Journal of Geophysical Research E: Planets, 2017, 122, 2510-2543.	3.6	95
44	OSIRIS-REx: Sample Return from Asteroid (101955) Bennu. Space Science Reviews, 2017, 212, 925-984.	8.1	426
45	The complex relationship between olivine abundance and thermal inertia on Mars. Journal of Geophysical Research E: Planets, 2016, 121, 1293-1320.	3.6	8
46	The meteorology of Gale crater as determined from rover environmental monitoring station observations and numerical modeling. Part I: Comparison of model simulations with observations. Icarus, 2016, 280, 103-113.	2.5	54
47	Compositional provinces of Mars from statistical analyses of TES, GRS, OMEGA and CRISM data. Journal of Geophysical Research E: Planets, 2015, 120, 62-91.	3.6	32
48	The OSIRISâ€REx target asteroid (101955) Bennu: Constraints on its physical, geological, and dynamical nature from astronomical observations. Meteoritics and Planetary Science, 2015, 50, 834-849.	1.6	168
49	Curiosity's rover environmental monitoring station: Overview of the first 100 sols. Journal of Geophysical Research E: Planets, 2014, 119, 1680-1688.	3.6	112
50	Terrain physical properties derived from orbital data and the first 360 sols of Mars Science Laboratory Curiosity rover observations in Gale Crater. Journal of Geophysical Research E: Planets, 2014, 119, 1322-1344.	3.6	43
51	Observations and preliminary science results from the first 100 sols of MSL Rover Environmental Monitoring Station ground temperature sensor measurements at Gale Crater. Journal of Geophysical Research E: Planets, 2014, 119, 745-770.	3.6	67
52	Characteristics of pebble―and cobbleâ€sized clasts along the Curiosity rover traverse from Bradbury Landing to Rocknest. Journal of Geophysical Research E: Planets, 2013, 118, 2361-2380.	3.6	44
53	Distribution and characteristics of Adirondack-class basalt as observed by Mini-TES in Gusev crater, Mars and its possible volcanic source. Icarus, 2012, 218, 917-949.	2.5	29
54	A search for basaltic-to-intermediate glasses on Mars: Assessing martian crustal mineralogy. Icarus, 2010, 210, 135-149.	2.5	32

#	Article	IF	CITATIONS
55	Thermal infrared (vibrational) spectroscopy of Mg–Fe olivines: A review and applications to determining the composition of planetary surfaces. Chemie Der Erde, 2010, 70, 7-33.	2.0	107
56	Seeking phyllosilicates in thermal infrared data: A laboratory and Martian data case study. Journal of Geophysical Research, 2009, 114, .	3.3	15
57	Global distribution, composition, and abundance of olivine on the surface of Mars from thermal infrared data. Journal of Geophysical Research, 2008, 113, .	3.3	189
58	Surface and craterâ€exposed lithologic units of the Isidis Basin as mapped by coanalysis of THEMIS and TES derived data products. Journal of Geophysical Research, 2008, 113, .	3.3	86
59	Visible, nearâ€infrared, and middle infrared spectroscopy of altered basaltic tephras: Spectral signatures of phyllosilicates, sulfates, and other aqueous alteration products with application to the mineralogy of the Columbia Hills of Gusev Crater, Mars. Journal of Geophysical Research, 2008, 113.	3.3	79
60	Evidence for extensive olivineâ€rich basalt bedrock outcrops in Ganges and Eos chasmas, Mars. Journal of Geophysical Research, 2008, 113, .	3.3	64
61	Chloride-Bearing Materials in the Southern Highlands of Mars. Science, 2008, 319, 1651-1654.	12.6	381
62	Visible to near-IR multispectral orbital observations of Mars. , 2008, , 169-192.		8
63	Global mineralogy mapped from the Mars Global Surveyor Thermal Emission Spectrometer. , 2008, , 193-220.		7
64	The compositional diversity and physical properties mapped from the Mars Odyssey Thermal Emission Imaging System. , 2008, , 221-241.		6
65	Geologic characteristics of relatively high thermal inertia intracrater deposits in southwestern Margaritifer Terra, Mars. Journal of Geophysical Research, 2007, 112, .	3.3	16
66	Characterization and petrologic interpretation of olivine-rich basalts at Gusev Crater, Mars. Journal of Geophysical Research, 2006, 111, n/a-n/a.	3.3	227
67	Evidence for locally derived, ultramafic intracrater materials in Amazonis Planitia, Mars. Journal of Geophysical Research, 2006, 111, .	3.3	8
68	Evidence for magmatic evolution and diversity on Mars from infrared observations. Nature, 2005, 436, 504-509.	27.8	177
69	Evidence for extensive, olivine-rich bedrock on Mars. Geology, 2005, 33, 433.	4.4	182
70	Discrimination of glass and phyllosilicate minerals in thermal infrared data. Journal of Geophysical Research, 2005, 110, n/a-n/a.	3.3	15
71	Mineralogy of Martian atmospheric dust inferred from thermal infrared spectra of aerosols. Journal of Geophysical Research, 2005, 110, .	3.3	58
72	Initial Results from the Mini-TES Experiment in Gusev Crater from the Spirit Rover. Science, 2004, 305, 837-842.	12.6	168

#	Article	IF	CITATIONS
73	Mineralogy at Meridiani Planum from the Mini-TES Experiment on the Opportunity Rover. Science, 2004, 306, 1733-1739.	12.6	370
74	Accuracy of plagioclase compositions from laboratory and Mars spacecraft thermal emission spectra. Journal of Geophysical Research, 2004, 109, .	3.3	27
75	Identification of quartzofeldspathic materials on Mars. Journal of Geophysical Research, 2004, 109, .	3.3	110
76	Morphology and Composition of the Surface of Mars: Mars Odyssey THEMIS Results. Science, 2003, 300, 2056-2061.	12.6	368
77	Thermal infrared emission spectroscopy of titanium-enriched pyroxenes. Journal of Geophysical Research, 2003, 108, .	3.3	7
78	Searching for the source regions of martian meteorites using MGS TES: Integrating martian meteorites into the global distribution of igneous materials on Mars. Meteoritics and Planetary Science, 2003, 38, 871-885.	1.6	157
79	Analysis of terrestrial and Martian volcanic compositions using thermal emission spectroscopy: 2. Application to Martian surface spectra from the Mars Global Surveyor Thermal Emission Spectrometer. Journal of Geophysical Research, 2001, 106, 14733-14746.	3.3	126
80	Analysis of terrestrial and Martian volcanic compositions using thermal emission spectroscopy: 1. Determination of mineralogy, chemistry, and classification strategies. Journal of Geophysical Research, 2001, 106, 14711-14732.	3.3	124
81	Mars Global Surveyor Thermal Emission Spectrometer experiment: Investigation description and surface science results. Journal of Geophysical Research, 2001, 106, 23823-23871.	3.3	903
82	A Global View of Martian Surface Compositions from MGS-TES. Science, 2000, 287, 1626-1630.	12.6	613
83	A thermal emission spectral library of rock-forming minerals. Journal of Geophysical Research, 2000, 105, 9735-9739.	3.3	326
84	Detection of crystalline hematite mineralization on Mars by the Thermal Emission Spectrometer: Evidence for near-surface water. Journal of Geophysical Research, 2000, 105, 9623-9642.	3.3	427
85	Thermal infrared emission spectroscopy of the pyroxene mineral series. Journal of Geophysical Research, 2000, 105, 9701-9716.	3.3	113
86	Determining the modal mineralogy of mafic and ultramafic igneous rocks using thermal emission spectroscopy. Journal of Geophysical Research, 2000, 105, 9717-9733.	3.3	106
87	Identification of a basaltic component on the Martian surface from Thermal Emission Spectrometer data. Journal of Geophysical Research, 2000, 105, 9609-9621.	3.3	250
88	Determination of Martian meteorite lithologies and mineralogies using vibrational spectroscopy. Journal of Geophysical Research, 1997, 102, 25593-25603.	3.3	79